energies

MDPI

Article

Application of Simulated Annealing Algorithm in Core Flow Distribution Optimization

Zixuan Wang, Yan Wang *, Haipeng Xu and Heng Xie

Institute of Nuclear and New Energy Technology, Tsinghua University, Beijing 100084, China
* Correspondence: wangyanfcw@tsinghua.edu.cn; Tel.: +86-10-62788157

Abstract: Core flow distribution is closely related to the thermal–hydraulic performance and safety of reactors. For natural circulation reactors with a limited driving force, flow distribution optimization is of particular significance, which can be contrived by suitably assigning the inlet resistance of a core assembly channel in reactor design. In the present work, core flow distribution optimization during the fuel life cycle is regarded as a global optimization problem. The optimization objective is to minimize the maximal outlet temperature difference of assembly channels during the fuel life cycle, while the input variable is the inlet resistance coefficient of each assembly channel. The simulated annealing algorithm is applied to the optimization code. The results show that the maximal outlet temperature difference is significantly reduced after optimization, and the resultant core outlet temperature distribution becomes more uniformed. Further evaluation indicates that the optimal solution has good applicability and stability under different reactor conditions. A comparison of the optimization objective function using different temperature difference definitions is also studied in the current study.

Keywords: flow distribution optimization; natural circulation; global optimization; simulated annealing algorithm

Citation: Wang, Z.; Wang, Y.; Xu, H.; Xie, H. Application of Simulated Annealing Algorithm in Core Flow Distribution Optimization. *Energies* **2022**, *15*, 8242. https://doi.org/10.3390/en15218242

Academic Editors: Jingen Chen and Yu Yu

Received: 21 September 2022
Accepted: 3 November 2022
Published: 4 November 2022

1. Introduction

The core flow distribution calculation is an important issue for nuclear reactor design, as it provides important input parameters for thermal–hydraulic analysis and safety analysis. A core flow distribution that matches well with the power distribution can flatten the temperature distribution at the core outlet and thus furnish a higher safety margin [1–3]. In a natural circulation reactor whose driving force is limited, the total flow of the primary loop and the flow into each fuel assembly channel are greatly affected by the resistance in the assembly channel [1]. Therefore, in the design of a natural circulation reactor, flow distribution optimization by means of reasonably arranging the resistance of the fuel assembly channels is of significant research value.

Recent years have seen three major methods applied to the numerical simulation of flow distribution. The first kind is the utilization of existing thermal–hydraulic analysis programs, such as the subchannel analysis code COBRA, which has been utilized to calculate the coolant flow distribution of a 900 MW PWR [4]. The second method is to make use of a computational fluid dynamics software (CFD), such as FLUENT or CFX5 [5,6]. Since existing programs or CFDs may not be applicable to flow distribution simulation under certain reactor design conditions, establishing a relevant thermal–hydraulic solution model and then developing a corresponding flow distribution optimization code based on the model is the third method [3].

On account of its significance in improving the safety and economy of natural circulation reactors, flow distribution optimization is a valuable area of research. A study on the core flow distribution of a small modular sodium-cooled fast reactor (SFR) revealed that the core flow distribution is determined by the core power distribution and the resistance of

the fuel assembly channel that is in common with it under natural circulation conditions [1]. Using the FLUENT code, Bae et al. simulated the inlet flow field distribution of the SMART reactor. The results showed that despite the non-uniformity in the flow rate discharged from upstream, the design of the lower core support plate achieved a reasonable distribution of the mass flow rate at the inlet [7]. Xu et al. developed an optimization code coupled with COBRA. A 200 MW natural circulation reactor with closed assemblies was chosen to be tested. The results indicated that the non-uniformity of the coolant temperature at the assembly channel outlet at atypical stages (beginning, middle, or end the of fuel life cycle) were improved after optimization [8]. Zhu et al. studied the flow distribution scheme of the SPALLER-100 reactor. A local optimal flow distribution calculation model was constructed, and the temperature difference at the core outlet under a certain power distribution was remarkably reduced [9].

However, during the fuel life cycle, as the core power distribution changes, the coolant temperature at the assembly channel outlets changes accordingly. Generally, the resistance scheme for the purpose of flow distribution optimization at a certain time node would not be optimal at other time nodes. Consequently, it is necessary to search for an optimal flow distribution scheme that can meet the optimization objective at multiple time nodes during a fuel life cycle. Based on the above considerations, core flow distribution optimization can be treated as a global optimization problem. From the previous literature review, it can be found that most of the studies in the field have focused on the maximum temperature difference at the assembly outlet, at which the theoretical solution during fuel life cycle is difficult to acquire but is of research significance. In view of this, modern metaheuristic algorithms that use the stochastic method are applied to the problem and generally make little or no assumptions on the structural characteristics of optimization problems [10]. In recent decades, several metaheuristic algorithms have been expanded to optimization problems in the nuclear field. The simulated annealing algorithm (SA) [11–13], the gravitational search algorithm (GSA) [14], and the grey wolf optimization algorithm (GWO) [15] have been introduced for the loading pattern optimization of pressurized water reactors (PWRs). Random forest (RF) was applied to the design of the recirculation pipeline flow resistance for an integrated small modular reactor [16]. It is noted that these metaheuristic algorithms have shown promising performance and should be proposed for other optimization problems in the nuclear engineering field [14]. As a modern metaheuristic algorithm with a high convergence speed and global optimal achievement, SA and improved SAs have been widely applied to reactor design optimization [11–13]. As a result, this paper applies SA to flow distribution optimization.

In the present work, the input variable of the optimization problem is a set of assembly inlet resistances, and the optimization objective is minimizing the maximal temperature difference at the assembly outlet ΔT_{max} during the fuel life cycle. Through combining SA with the COBRA code, which is used to conduct the thermal–hydraulic calculation, the global flow distribution optimization code is developed. A 200 MW natural circulation reactor is chosen to test the code. Furthermore, to test the applicability and stability of the SA solution, ΔT_{max} and MDNBR (minimum departure nucleate boiling ratio) are calculated at different total thermal powers, coolant inlet temperatures, total flows, and lower limits of the inlet resistance coefficient. Finally, the objective function results under two different definitions of ΔT_{max} are compared and analyzed.

2. Process on Core Flow Distribution Optimization during Fuel Life Cycle

2.1. Optimization Model

The research object of this study is a natural circulation light water reactor with closed fuel assemblies, and the core can be described as having a disconnected parallel channel model (Figure 1). The geometric parameters of the parallel channels are identical. As the coolant passes through the core in the axial direction, there is no bypass flow and no radial heat transfer. Therefore, a one-dimensional heat transfer flow model is adopted [8].

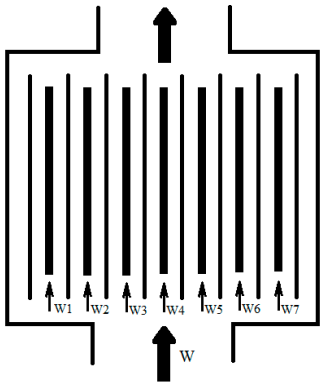

Figure 1. Schematic diagram of closed parallel channel.

The flow distribution is jointly determined by the power distribution and local resistance. In real reactor design, a practicable approach to obtaining the expected flow rate is achieved by adjusting the inlet resistance by installing different throttle orifices at the channel inlet [1,3]. In this study, the input variable of the optimization problem is the coefficient of inlet resistance (*CR*) of each assembly channel, which represents the resistance. It is noteworthy that the total flow *W* of the primary loop should be maintained no lower than a certain value according to the requirements of the thermal–hydraulic design. Resultantly, *CR* has an upper limit. Meanwhile, *CR* has a lower limit owing to the inlet's inherent local resistance of the assembly channel. A fixed *W* that can satisfy the design requirements is presumed for reasonable simplification. For global optimization problems whose input variable has certain upper and lower limits, it can be described as follows:

$$\begin{array}{l} \text{Minimize } f(CR_1, \cdots, CR_n) = \min\{\Delta T_{tn,1}, \cdots, \Delta T_{tn,j}, \cdots, \Delta T_{tn,m}\} \\ \text{Subject to } CR_{i,\min} \le CR_i \le CR_{i,\max}, i = 1, 2, \cdots, n; W = \text{const} \end{array} \quad (1)$$

where CR_i is the inlet resistance of ith each channel, $\Delta T_{tn,j}$ is the $\Delta T_{\max}$ at the jth time node of the fuel life cycle, and $CR_{i,\min}$ and $CR_{i,\max}$ are the upper and lower limits of CR_i respectively. $\Delta T_{\max}$ at certain time nodes can be defined in the following two ways:

$$\begin{array}{r} \text{First definition: } \Delta T_{\max,1} = T_{\text{hottest}} - T_{\text{coolest}} \\ \text{Second definition: } \Delta T_{\max,2} = T_{\text{hottest}} - T_{\text{ave}} \end{array} \quad (2)$$

where T_{hottest} is the highest coolant temperature at the assembly outlet, T_{coolest} is the lowest coolant temperature at the assembly outlet, and T_{ave} is the average coolant temperature at the assembly outlet.

The first definition of $\Delta T_{\max}$ is conducive to flattening the core temperature distribution so that the efficiency of reactor can be enhanced. The second contributes to limiting the highest coolant temperature at the assembly outlets, and the reactor's safety margin will be improved as a result.

The code used in this study for sub-channel calculation is COBRA IIIC, written in the Fortran language. Using a mathematical model that considers both turbulent and diversion crossflow mixing between adjacent subchannels, COBRA IIIC can compute the flow and enthalpy in rod–bundle nuclear fuel element subchannels in both steady and transient states. It is assumed that the flow in each assembly channel is one-dimensional, two-phase, separated, and slip-flow. Steady state two-phase flow correlations are assumed to apply to transients. COBRA IIIC proposes a semi-explicit finite difference method to solve the equations in the mathematical model. Through this method, a boundary-value flow solution for both the steady and transient states can be obtained. The boundary conditions are the inlet enthalpy, inlet mass velocity, and exit pressure. In the current version, the input is simple and flexible. By means of integrating coarse grids with fine grids, the thermal–hydraulic analysis of the whole core can be executed. Given that the lateral momentum

equation can be applied to the calculation, the fine subchannel model analysis can be contrived. Moreover, the same pressure drop can be maintained between components under heating conditions for different iterations. As a consequence, the flow distribution calculation between assemblies is realized [17,18]. Additionally, some modifications and supplements are made to the original COBRA IIIC code so that the research requirements of this paper can be satisfied. Table 1 presents the thermal–hydraulic formulation of this study.

Table 1. Basic thermal–hydraulic models used in the COBRA code.

Model		
Single-phase friction model		$f = a\mathrm{Re}^b + c$, without wall viscosity correction *
Two-phase friction model		Armand correlation
Void fraction model	Subcooled void model	Levy-subcooled void correlation
	Slip ratio model	Smith slip ratio correlation
Critical heat flux correlation		Modified Barnett correlation

* where a, b, and c are specified constants that depend on the subchannel roughness and geometry; Re is the Reynold's number.

2.2. Simulated Annealing Algorithm

SA is a metaheuristic algorithm that is used to approximate the global optimum of a given function in a large search space. To be specific, SA adopts iterative movement on the basis of the variable temperature parameter that simulates the transaction of annealing in metallurgy. A simple optimization algorithm, such as Gradient Descent, would be stuck in situations in which there are a lot of local minima or maxima. On the contrary, SA proposes an efficacious solution to problems by using the value of the objective function rather than the gradient of the function. SA combines the Metropolis rule with the cooling procedure for the annealing process. The ideology of the Metropolis rule is to conduct extra searches the neighborhood of the solution of the previous step. Meanwhile, the searching process is random [11–13]. Specifically, for a current optimization problem, let us consider x_old as the candidate solution of the objective function $f(x_i)$ and define $\Delta f = f(x\_new) - f(x\_old)$, where x_new is a new solution randomly taken from its neighborhood. If $\Delta f \leq 0$, then take x_new as a new candidate; otherwise, judge whether $\exp(-\Delta f / T_i) > random(0,1)$, where T_i is the current temperature parameter. If so, then also accept x_new as a new candidate; otherwise, reject it and go back to the previous candidate. As we can see from the above search process, the Metropolis rule allows the current step to somewhat jump out of the previous candidate solution, even if the value of the new objective function is becoming worse.

When it comes to the specific application of SA in current optimization problems, first, a relatively higher temperature parameter is taken, and then, the temperature parameter undergoes a decrease that imitates the annealing process of the metals. At each annealing temperature parameter, the procedure is repeated until the system reaches the steady state, which includes the generation of a new candidate solution, the calculation of the value of the new solution's objective function, and the judgement of whether to accept the new solution or not. The search process will not be discontinued unless the temperature parameter decreases to the lower limit or unless the objective function value is satisfied.

Figure 2 presents the flow chart of the optimization code based on SA. The detailed procedures are described as follows:

1. Generate an initial solution x_old stochastically whose objective function $f(x\_old)$ is then calculated via COBRA; determine T_0 (the initial annealing temperature) and L (the maximal search times, also called the Markov chain length, a constant during optimization); set $k = 0$ (searching times at the current temperature);
2. If $k \geq L$, go to step 3; otherwise, a new solution x_new is randomly taken from the neighborhood of x_old; then, let $\Delta f = f(x\_new) - f(x\_old)$. If $\Delta f \leq 0$, then accept

x_new as the new candidate; otherwise, judge whether $\exp(-\Delta f / T_i)$ is larger than a random number between (0, 1). If so, then also accept x_new as a new candidate; otherwise, reject and go back to x_old. After the check of the candidate solution is accomplished, make $k = k + 1$ and repeat step 2;

3. In order to decrease the temperature parameter, let $T_{i+1} = d(T_i)$. Terminate the cooling procedure for the annealing process if the stop condition is satisfied; otherwise, go back to step 2;
4. After the global optimal scheme of *CR* is searched, check whether MDNBR is lower than a certain value. If not, *CR* is supposed to be adjusted until the thermal–hydraulic safety requirement is satisfied;
5. Output the optimization results.

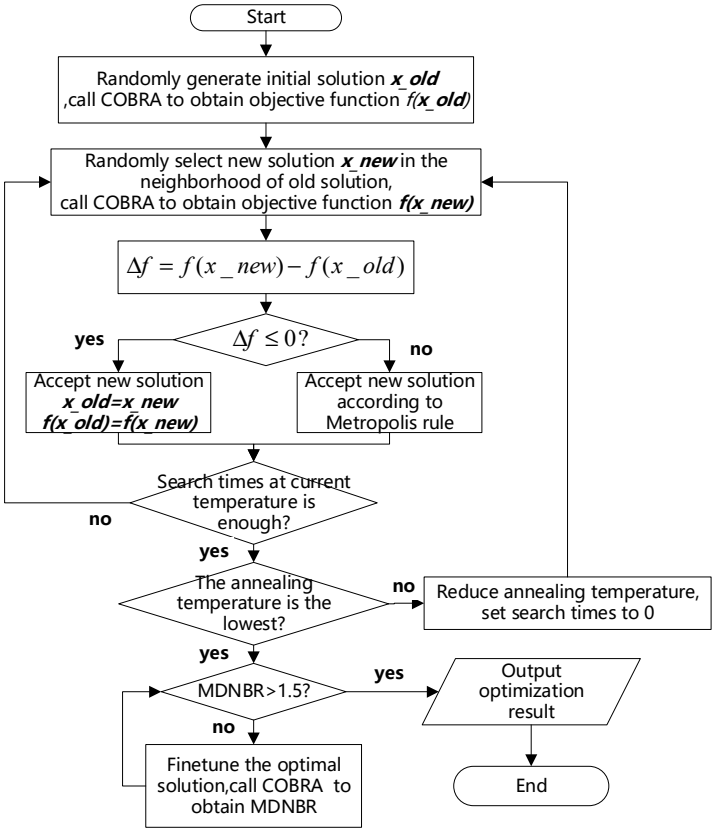

Figure 2. Flow chart of optimization code based on SA.

3. Results and Analysis of Core Flow Distribution Optimization Code

In this section, a 200 MW natural circulation reactor is selected for analysis. There are 208 closed fuel assemblies. The primary pressure of the reactor in operation is 8 MPa, and the saturation temperature of the corresponding coolant is 295 °C. The coolant temperature at the assembly inlet is 230 °C. The fuel life cycle of the reactor core is about 650 days. The main parameters of the reactor are given in Table 2. As a result of geometric symmetry, only one quarter of the reactor core (including 52 fuel assembly channels) is modeled for analysis.

$\Delta T_{\max,1}$ was chosen as the optimization objective to conduct preliminary calculations. The entire fuel life cycle is evenly divided with an interval of 50 days, forming a total of 14 typical time nodes. It is noteworthy that without design optimization, there is no throttle orifice installed at the channel inlet, and the *CR* of each assembly channel is equal to 7.9 (the lower limit of *CR* under the current reactor design).

Table 2. Main parameters of the tested reactor.

Parameters	Value
Total thermal power (MW)	200.0
System pressure (MPa)	8.0
Total mass flow (kg/s)	943.5
Coolant temperature at the assembly inlet (°C)	230
Number of assembly channels	208
Fuel core life (day)	650

3.1. Optimization Results

3.1.1. Parameters Choices of SA

The optimization effect of SA depends on parameter selection, which mainly includes an initial annealing temperature T_0, new solution generation method, temperature attenuation method, and maximum search times at each temperature L. In this paper, a sensitivity analysis of these parameters is studied to obtain an optimal set of parameters.

T_0 is determined first. Figure 3 sketches the relationship between T_0 and the acceptance probability of the worse solution. In the present work, the acceptance probability at the beginning of the algorithm is set as 80%, and correspondingly, T_0 is equal to 1.2.

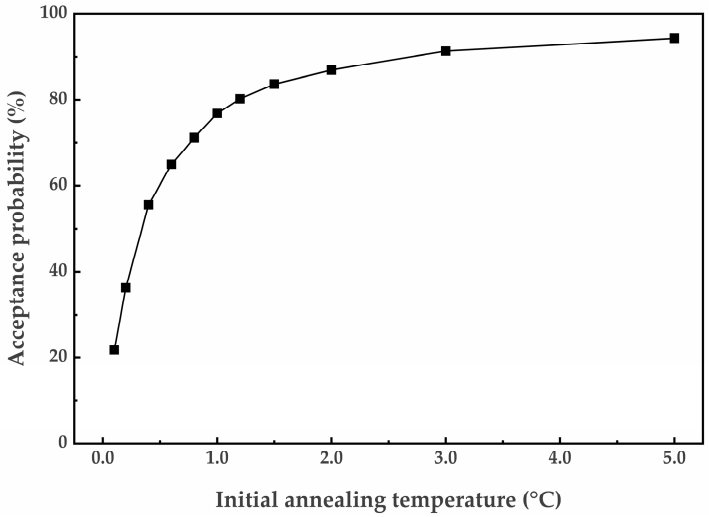

Figure 3. Relationship between initial annealing temperature and acceptance probability of worse solution.

The input variable CR is a positive continuous variable. In the case of dynamically adjusting the neighborhood size, the new solution generation method is:

$$x_{i+1} = (1 + \lambda \cdot r)x_i \tag{3}$$

where x_{i+1} is the new solution, and x_i is the old solution; λ is a coefficient that determines the neighborhood size; and r is a random number between $(-1, 1)$.

Table 3 lists the optimization results under different λ. Under equivalent calculation times, optimization cannot be achieved well when the neighborhood size is too big or too small. When λ is equal to 0.03, the optimal objective function value (9.27 °C) is obtained.

The temperature attenuation function is given as

$$T_{i+1} = \alpha \times T_i \tag{4}$$

where α is the temperature attenuation coefficient, and T_{i+1} is the attenuated temperature.

The optimization effect is jointly determined by α and L, where α is generally chosen to be between [0.9, 1.0], and L should be selected according to the actual problem. The opti-

mization results under different α and L are presented in Table 4. After the comprehensive comparison of the optimization effect and calculation times, α and L are set as 0.9 and 500, respectively, in the current work. Based on the above discussion, the final SA parameters selected for this case are listed in Table 5.

Table 3. Optimization results under different λ.

λ	Objective Function Value (°C)	Calculation Times
0.01	9.40	23,000
0.03	9.27	23,000
0.05	9.65	23,000
0.1	10.25	23,000

Table 4. Optimization results under different α and L.

α	L	Objective Function Value (°C)	Calculation Times
0.9	500	9.27	23,000
0.92	500	9.28	29,000
0.95	300	9.22	29,000
0.99	100	9.36	47,000
0.999	5	9.30	23,930
0.9999	1	9.27	47,865

Table 5. Parameters of SA.

Parameters	Value
Initial annealing temperature T_0 (°C)	1.2
Neighborhood size coefficient λ	0.03
Temperature attenuation coefficient α	0.9
Maximal searching times at each annealing temperature L	500

3.1.2. Results of SA Solution

The results show that the temperature difference at the assembly outlets under the obtained optimal solution decreases obviously at almost all typical stages compared to the case without optimization. Figure 4 gives a CR of 52 assembly channels in the optimal solution. They are both greater than the lower limit of CR (7.9), and the average value of CR is 14.26. Figure 5 shows that the $\Delta T_{\max,1}$ during fuel life cycle is 9.27 °C, which decreases by 46.5% compared to the value without optimization (17.33 °C). Meanwhile, the maximal outlet temperature of the module is 279.90 °C, and MDNBR is 3.221. They both meet the safety limit requirements. Therefore, the feasibility of the code based on SA is proven.

3.2. Applicability and Stability of Optimization Solution

In order to evaluate the applicability and stability of the optimal solution of SA, the above optimal solution is tested in cases in which certain selected typical conditions change, such as the total thermal power, the coolant temperature at the assembly inlet, the total flow, and the lower limit of CR. The change in the total thermal power, the coolant temperature at the assembly inlet, and the total flow will influence local highest temperature, and an excessive assembly temperature may endanger core safety. When it comes to the lower limit of CR, a smaller lower limit means that a better solution may be found in a larger domain. Thus, these parameters are considered to be key factors for the evaluation of the optimal solution.

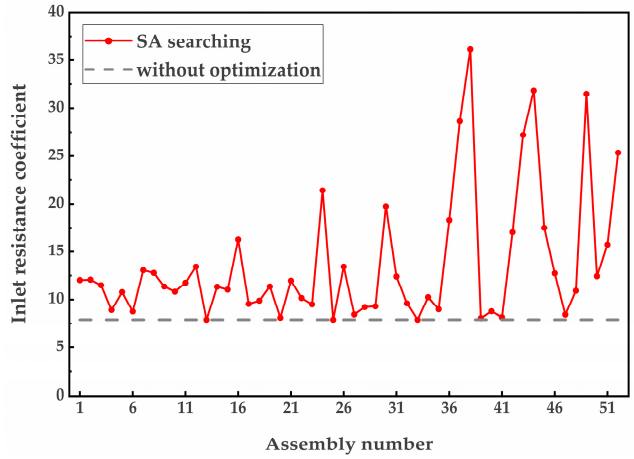

Figure 4. Inlet resistance coefficient of optimal solution.

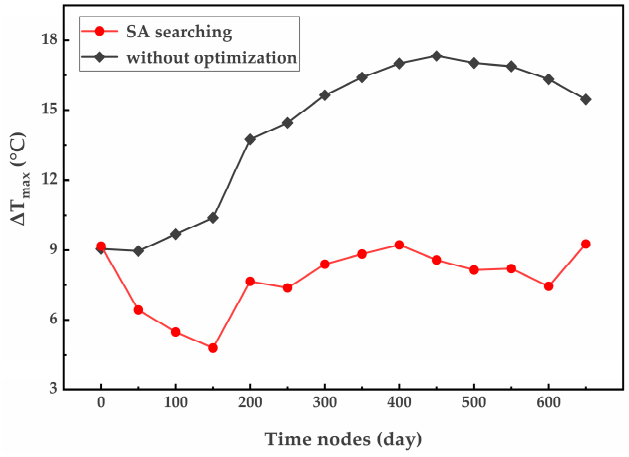

Figure 5. Outlet coolant temperature difference during single fuel life cycle.

3.2.1. Total Thermal Power

The total thermal power is increased by 2.5%, 5%, 7.5%, 10%, 12.5%, and 15%. Under the corresponding power, $\Delta T_{max,1}$ and MDNBR are calculated using the SA solution for the initial conditions. Figure 6 shows that as the total thermal power is raised, $\Delta T_{max,1}$ increases to a small extent, while MDNBR decreases slightly. When the core thermal power is increased to 115% of the initial value, $\Delta T_{max,1}$ only increases by 0.81 °C; MDNBR is 2.784, which still satisfies the safety requirements. These results illustrate that the optimal solution calculated by SA has good stability in the case of changing the total thermal power.

3.2.2. Coolant Temperature at the Assembly Inlet

The coolant temperature at the assembly inlet is increased from 230 °C to 232.5 °C, 23 5 °C, 237.5 °C, 240 °C, 242.5 °C, and 245 °C. Under the corresponding temperatures, $\Delta T_{max,1}$ and MDNBR are calculated using the SA solution for the initial conditions. From Figure 7, it is clear that the change in $\Delta T_{max,1}$ and MDNBR is minor as the coolant temperature increases. When the coolant temperature is increased by 15 °C, $\Delta T_{max,1}$ changes from 9.27 °C to 8.87 °C; MDNBR is 3.159, which still meets the safety requirements. These results indicate that the optimal solution calculated by SA has good stability in the case of changing the coolant temperature at the assembly inlet.

3.2.3. Total Flow of the Loop

The total flow of the loop is changed by −10%, −5%, 5%, and 10%. Under the corresponding total flows, $\Delta T_{max,1}$ and MDNBR are calculated by using the SA solution

for the initial conditions. As shown in Figure 8, when the total flow changes within the range, the optimization effect is always acceptable, and MDNBR still meets the safety requirements. Therefore, the optimal solution calculated by SA has good stability in the case of changing the total flow.

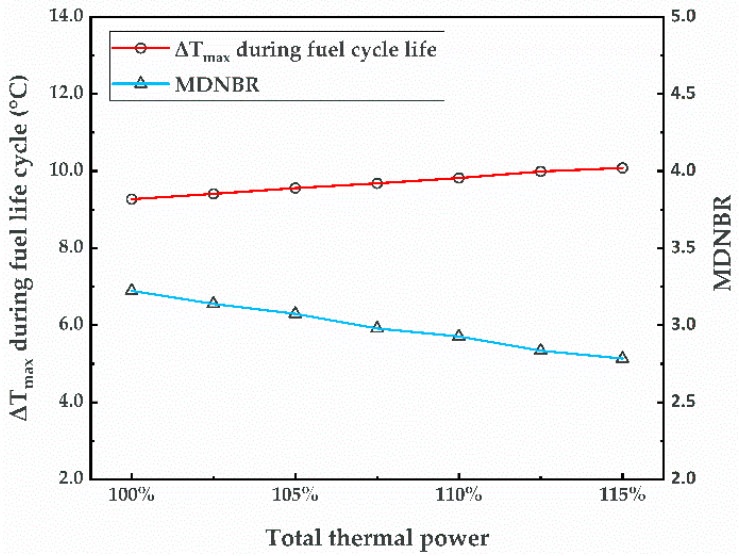

Figure 6. Optimization results under different total thermal powers.

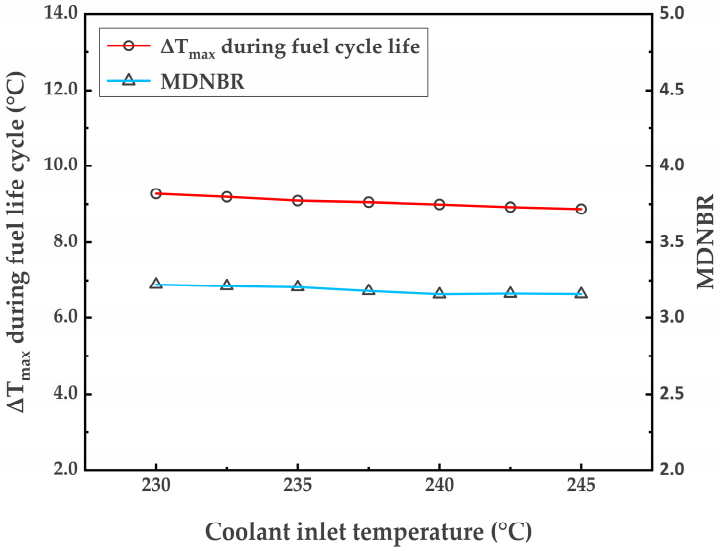

Figure 7. Optimization results under different assembly inlet temperatures.

3.2.4. Lower Limit of CR

In the former cases, the lower limit of *CR* is 7.9 as a no-throttle orifice is installed at the core inlet. In fact, this value is expected to be smaller and to have a reasonable structural design or an optimized manufacturing technique for the channel inlet. In this section, a theoretical study on the influence of a smaller lower limit is conducted. Flow distribution schemes under different lower limits (3.9, 5.9 and 7.9) are optimized and compared. Figure 9 presents the *CR* of 52 assembly channels under different lower limits. It can be seen that the characteristics of the distribution of *CR* are consistent. Meanwhile, $\Delta T_{max,1}$ decreases from 9.27 °C to 8.70 °C during the fuel life cycle (Figure 10), and thus, a better optimization effect is achieved. This is because the domain of definition of *CR* is enlarged when the lower limits are decreased, and a better optimal solution is more likely to be found in a larger search domain.

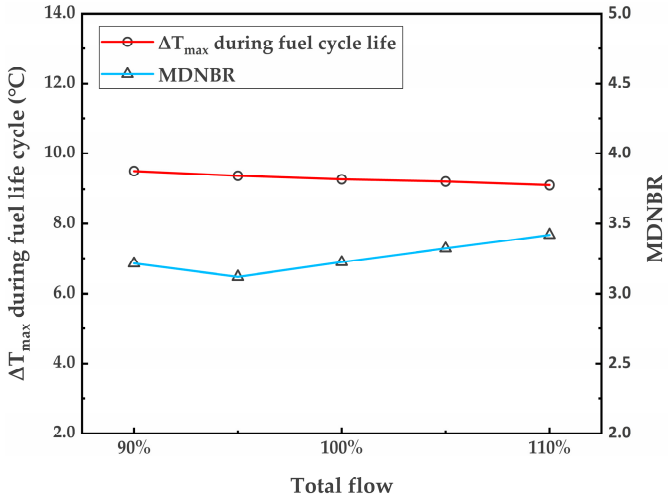

Figure 8. Optimization results under different total flows.

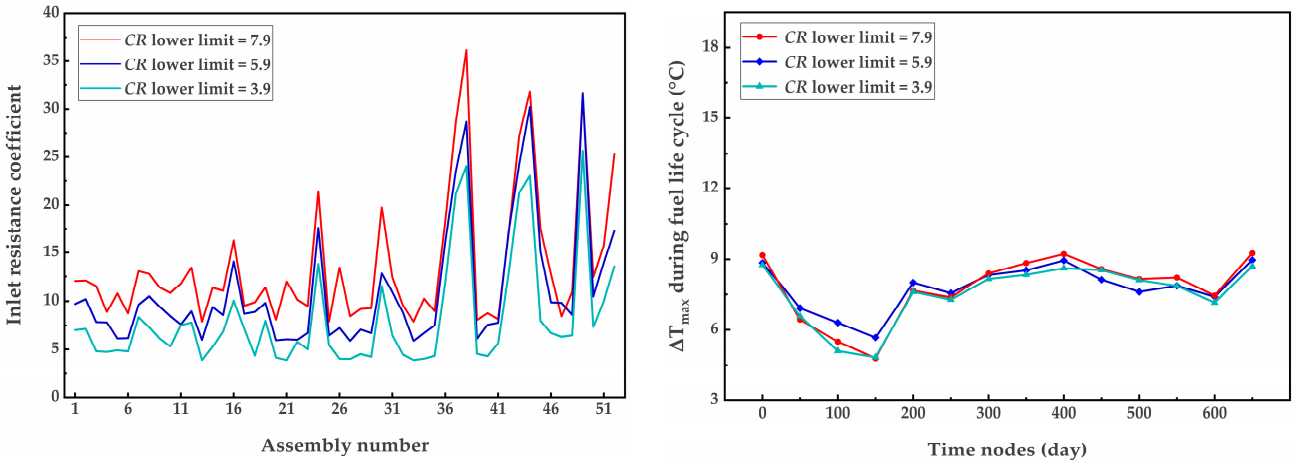

(**a**) (**b**)

Figure 9. (**a**) Assembly inlet resistance coefficient schemes under three different lower limits; (**b**) $\Delta T_{max,1}$ during fuel life cycle under three different lower limits.

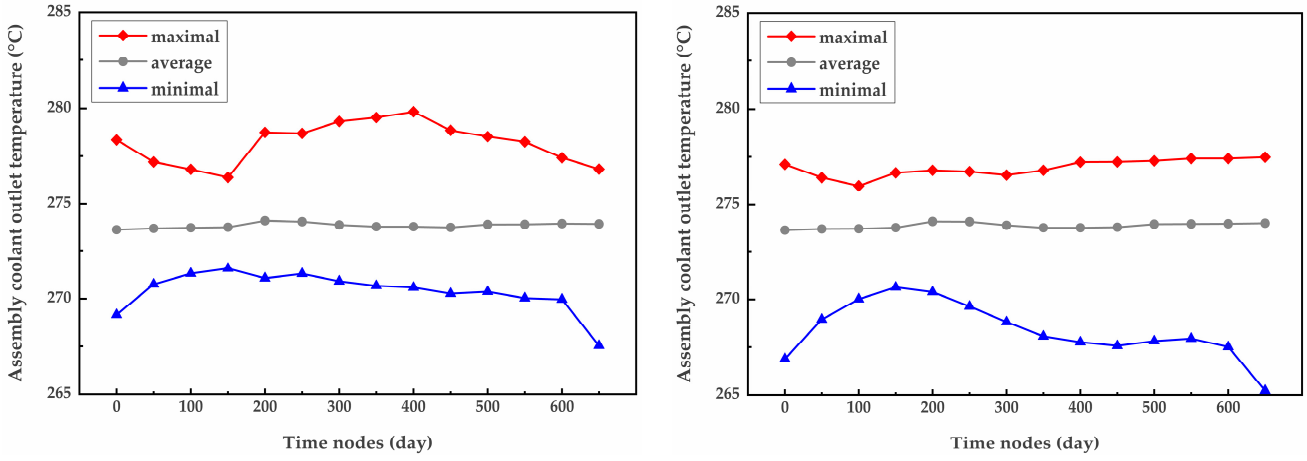

(**a**) (**b**)

Figure 10. (**a**) Optimization effects when ΔT_{max} is defined as $\Delta T_{max,1}$; (**b**) optimization effects when ΔT_{max} is defined as $\Delta T_{max,2}$.

3.3. Comparison of Optimization Objective Function Using Different Temperature Differences

In the above tests, the first definition of ΔT_{max} is used to flatten the temperature distribution. In order to decrease the highest coolant temperature of all of the assembly channel outlets, the second type is proposed. The comparison of the optimization effects of the two kinds of temperature differences are listed in Table 6. It can be seen that the optimization based on $\Delta T_{max,1}$ can decrease the difference between the highest outlet temperature and the lowest outlet temperature from 17.33 °C to 9.27 °C, while the optimization method based on $\Delta T_{max,2}$ can decrease the difference between the highest outlet temperature and the average outlet temperature from 6.79 °C to 3.47 °C.

Table 6. Comparison of optimization effects of two temperature differences.

	$\Delta T_{max,1}$ (°C)	$\Delta T_{max,2}$ (°C)	MDNBR (After Optimization)
without optimization	17.33	6.79	3.223
$\Delta T_{max} = \Delta T_{max,1}$	9.27	6.03	3.223
$\Delta T_{max} = \Delta T_{max,2}$	12.26	3.47	3.336

For further evaluation, the highest, the average, and the lowest coolant temperatures at the outlet of 52 assembly channels at the 14 typical time nodes under the two definitions of temperature difference are compared. The optimization results based on $\Delta T_{max,1}$ show that the difference between the highest outlet temperature and the lowest outlet temperature is lower (Figure 10a). Accordingly, the outlet coolant temperature distribution is better flattened, which is conducive to improving the efficiency of the reactor's thermal–hydraulic design. The optimization results based on $\Delta T_{max,2}$ show that the highest outlet temperature is relatively lower (Figure 10b). Thus, defining ΔT_{max} as $\Delta T_{max,2}$ can result in further safety protection for reactor design during distribution optimization.

As shown in the above figures, in both cases, the highest coolant temperature of all of the assembly channel outlets is much lower than the saturation temperature (295 °C) under normal operation conditions. Given that both cases can provide safety protection, the optimization based on $\Delta T_{max,1}$ is supposed be a better choice, resulting in improved thermal efficiency in the reactor design.

4. Conclusions

For natural circulation reactors, an optimized core flow distribution aimed at better matching the core power distribution contributes to promoting reactor performance and safety. In this paper, global SA optimization is applied to flow distribution optimization in a natural circulation reactor core, where ΔT_{max}, the *CR* of the assembly channel, and MDNBR are considered as the objective function, input variable, and thermal hydraulics safety criterion, respectively. The results show that the algorithm has a significant effect on decreasing the maximal outlet temperature difference, which is reduced from 17.33 °C (without optimization) to 9.27 °C. Parameters that may influence the optimization effect and thermal safety are changed for further evaluation, such as the total thermal power, the coolant temperature at the assembly inlet, the total flow, and the lower limit of *CR*. Additionally, the analysis results indicate that the optimal solution calculated by SA has good applicability and stability. Furthermore, the optimization values of the objective function using different definitions of temperature difference are compared. The optimization objective based on $\Delta T_{max,1}$ can contribute to improving the efficiency of the reactor's thermal–hydraulic design, while the optimization objective based on $\Delta T_{max,2}$ will supply further safety protection for the reactor design during distribution optimization. In future work, optimization codes based on more different stochastic algorithms, such as the genetic algorithm (GA) and the characteristic statistic algorithm (CSA), will be studied and compared.

Author Contributions: Conceptualization, Y.W.; methodology, H.X. (Haipeng Xu) and Z.W.; software, Z.W. and H.X. (Haipeng Xu); validation, Z.W.; data curation, Z.W.; writing—original draft preparation, Z.W. and H.X. (Haipeng Xu); writing—review and editing, Y.W. and Z.W.; supervision, Y.W. and H.X. (Heng Xie); project administration, Y.W. and H.X. (Heng Xie); funding acquisition, Y.W. and H.X. (Heng Xie). All authors have read and agreed to the published version of the manuscript.

Funding: This work is supported by LingChuang Research Project of China National Nuclear Corporation.

Data Availability Statement: Not applicable.

Conflicts of Interest: The authors declare no conflict of interest.

References

1. Chen, Z.; Zhao, P.; Zhou, G.; Chen, H. Study of core flow distribution for small modular natural circulation lead or lead-alloy cooled fast reactors. *Ann. Nucl. Energy* **2014**, *72*, 76–83. [CrossRef]
2. Tian, W.; Qiu, S.Z.; Guo, Y.; Su, G.; Jia, D.; Liu, T.; Zhang, J. The calculation of mass flux distribution of CARR. *Chin. J. Nucl. Sci. Eng.* **2005**, *2*, 137–142.
3. Li, Z.; Zhou, T.; Sun, C. Code research on mass flux assignment of supercritical water-cooled reactor. *Nucl. Power Eng.* **2011**, *3*, 52–57.
4. Liang, C. Thermal Hydraulics Analysis and Primary Circuit System Numerical Simulation on Core and Water Hammer Characteristics of 900MW PWR. Master's Thesis, North China University of Water Resources and Electric Power, Zhengzhou, China, 2014.
5. Liu, B.; Jing, Y. Calculation and analysis of three-dimensional flow field in lower chamber of AP1000 reactor. *Nucl. Power Eng. Technol.* **2009**, *2*, 93–102.
6. Wang, J.; Bo, H.; Zheng, W.; Jiang, S. Flow distribution in a pool type reactor with plate fuel assemblies. *J. Tsinghua Univ. Sci. Technol.* **2004**, *6*, 754–757.
7. Bae, Y.; Kim, Y.I.; Park, C.T. CFD analysis of flow distribution at the core inlet of SMART. *Nucl. Eng. Des.* **2013**, *258*, 19–25. [CrossRef]
8. Xu, H.; Wang, Y.; Xie, H. A preliminary analysis on optimization of core flow distribution. *Prog. Nucl. Energy* **2022**, *146*, 104147. [CrossRef]
9. Zhu, E.; Chen, Q.; Zhao, P.; Zhao, Y.; Sun, Y.; Liu, Z.; Yu, T. Research on multi-objective optimization method for flow distribution of natural circulation reactor during its life-cycle. *Ann. Nucl. Energy* **2022**, *176*, 109266. [CrossRef]
10. Shen, P. *Global Optimization Method*, 1st ed.; China Science Publishing & Media Ltd.: Beijing, China, 2006.
11. Mahlers, Y.P. Core loading pattern optimization based on simulated annealing and successive linear programming. *Ann. Nucl. Energy* **1995**, *22*, 29–37. [CrossRef]
12. Hedayat, A. Developing a practical optimization of the refueling program for ordinary research reactors using a modified simulated annealing method. *Prog. Nucl. Energy* **2014**, *76*, 191–205. [CrossRef]
13. Tran, V.P.; Phan, G.T.T.; Hoang, V.K.; Ha, P.N.V.; Yamamoto, A.; Tran, H.N. Evolutionary simulated annealing for fuel loading optimization of VVER-1000 reactor. *Ann. Nucl. Energy* **2021**, *151*, 107938. [CrossRef]
14. Aghaie, M.; Mahmoudi, S.M. A novel multi objective Loading Pattern Optimization by Gravitational Search Algorithm (GSA) for WWER1000 core. *Prog. Nucl. Energy* **2016**, *93*, 1–11. [CrossRef]
15. Naserbegi, A.; Aghaie, M. PWR core pattern optimization using grey wolf algorithm based on artificial neural network. *Prog. Nucl. Energy* **2020**, *129*, 103505. [CrossRef]
16. Xiong, Q.; Shen, Y.; Dang, G.; Qiu, Z.; Deng, J.; Du, P.; Ding, S.; Wu, Z. Design for ACP100 long term cooling flow resistance with random forests and inverse quantification. *Ann. Nucl. Energy* **2023**, *180*, 109477. [CrossRef]
17. Jackson, J.W.; Todreas, N.E. *COBRA IIIC/MIT-2: A Digital Computer Program for Steady State and Transient Thermal-Hydraulic Analysis of Rod Bundle Nuclear Fuel Elements*; Energy Laboratory Report No: MIT-EL 81-018; Massachusetts Institute of Technology: Cambridge, MA, USA, 1981.
18. Loomis, J.N. *Reactor Thermal-Hydraulic Analysis Improvement and Application of the Code COBRA-IIIC/MIT*; Massachusetts Institute of Technology: Cambridge, MA, USA, 1981.